

Wet-chemical etching of FIB lift-out TEM lamellae for damage-free analysis of 3-D nanostructures

Emily M. Turner^{a,*}, Keshab R. Sapkota^b, Christopher Hatem^c, Ping Lu^b, George T. Wang^b, Kevin S. Jones^a

^a Materials Science and Engineering, University of Florida, Gainesville

^b Sandia National Laboratories, Albuquerque, NM

^c Applied Materials, Inc., Gloucester, MA

ARTICLE INFO

Keywords:

3-d nanostructure analysis

Wet etching

FIB cross section

Ion beam damage

ABSTRACT

Reducing ion beam damage from the focused ion beam (FIB) during fabrication of cross sections is a well-known challenge for materials characterization, especially cross sectional characterization of nanostructures. To address this, a new method has been developed for cross section fabrication enabling high resolution transmission electron microscopy (TEM) analysis of 3-D nanostructures free of surrounding material and free of damage detectable by TEM analysis. Before FIB processing, nanopillars are encapsulated in a sacrificial oxide which acts as a protective layer during FIB milling. The cross sectional TEM lamella containing the nanopillars is then mounted and thinned with some modifications to conventional FIB sample preparation that provide stability for the lamella during the following wet-chemical dip etch. The wet-chemical etch of the TEM lamella removes the sacrificial oxide layer, freeing the nanopillars from any material that would obscure TEM imaging. Both high resolution TEM and aberration corrected scanning TEM images of Si/SiGe pillars with diameters down to 30 nm demonstrate the successful application of this approach.

1. Introduction

While the focused ion beam (FIB) has been used for many applications ranging from micromachining [1,2] to tomographic characterization [3,4], the most common use is arguably the fabrication of samples for transmission electron microscopy (TEM) [5-9]. The powerful ability to fabricate site-specific cross sectional samples without destroying a large portion of the surrounding material via the FIB in situ lift-out method has proven especially useful in the microelectronics industry [10-14]. However, as dimensions decrease and complexity increases in modern day electronic devices, additional challenges arise in cross sectional TEM characterization. In particular, the characterization of 3-D nanostructures such as those used in quantum emitters [15], sensing applications [16], and vertical transistors [17-19] is problematic due to the nanometer scale size of these structures. This makes it difficult to capture 3-D nanostructures in a FIB lift-out lamella without either ion beam damage to the nanostructures during thinning or the unwanted presence of obscuring material in front of and behind the nanostructure if the operator chooses to avoid damage by not thinning all the way down to the 3-D nanostructures. While the

challenge of removing or minimizing the damage layer caused by ion beam milling has been largely addressed in bulk material cross section fabrication, attempts to minimize or remove the damage layer on 3-D nanostructure cross sections have not yet been reported. This challenge, particularly in the face of the prolific use of 3-D nanostructures, requires a novel approach to prevent damage to the sample of interest while enabling high resolution imaging through electron transparent TEM lamellae.

The damage layer introduced to the TEM cross section by the ion beam during thinning of the lamella is one of the universal challenges in FIB lift-out specimens [20]. The damaged layers sandwich the specimen, resulting in a 2-D projection of the sample that contains both amorphous and crystalline material. The phase distortion caused by the amorphous layers in the electron wave propagating through the sample in high resolution (phase contrast) TEM micrographs causes a loss of information about the embedded crystalline region of interest [21]. Scanning transmission electron microscopy (STEM), while less affected by sample thickness issues and amorphous damage layers, still suffers from an increase in background noise due to electron scattering from the amorphous layers sandwiching the crystalline material [22,23].

* Corresponding author.

E-mail addresses: emilyturner@ufl.edu (E.M. Turner), krsapko@sandia.gov (K.R. Sapkota), christopher_hatem@amat.com (C. Hatem), plu@sandia.gov (P. Lu), gtwang@sandia.gov (G.T. Wang), kjones@eng.ufl.edu (K.S. Jones).

<https://doi.org/10.1016/j.ultramic.2020.113049>

Received 18 February 2020; Received in revised form 7 June 2020; Accepted 10 June 2020

Available online 17 June 2020

0304-3991/ © 2020 Elsevier B.V. All rights reserved.

These amorphous layers also increase the STEM probe size thus reducing image resolution. Therefore, in the interest of high resolution S/TEM images it is desirable to eliminate as much of the amorphous material surrounding crystalline samples as possible.

There are several approaches to minimize or remove this layer, including careful ion beam thinning using successively lower ion beam voltages [24]. In many cases this allows the fabrication of TEM lamellae with damage layer thicknesses of down to approximately 2 nm on each side. Another approach has employed wet etching to remove the amorphous damage layers from the sidewalls of TEM specimens made using the trench method [25]. This wet etch removes the entire damage region, leaving the lamella without layers of amorphous damaged material that reduces the resolution of TEM analysis. However, the FIB trench method that was necessary to keep these lamellae stable during the wet etch is somewhat destructive to the sample and does not allow the fabrication of multiple FIB lamellae from the same area of the sample. Plasma etching [26] and Ar⁺ milling [27] have also been successful in reducing the damage layers inherent in FIB processing. However, these methods do not address the issues around structures that are 3-D (such as vertical wires) as opposed to 2-D (such as fins) or bulk materials.

To view these 3-D nanostructures in cross section via the FIB lift-out method, two options are currently available during the thinning process. The first option is to thin the TEM lamella until it is the thickness of the 3-D nanostructure, removing the material in front of and behind the nanostructure. However, this does not work for circular structures like vertical nanowires, where the edges of the structure will still have unwanted surrounding material. In addition, accurately capturing sub-100 nm structures in the thinnest part of the lamella requires a high skill level and even then may require several attempts before successful capture of the nanostructures. Further, these structures are small enough that even a 2 nm damage layer on each side becomes significant in reducing resolution. The second option is to only partially thin away the material, such as a protective carbon coating or a layer of electron beam deposited FIB platinum, surrounding the nanostructure. While this ensures damage to the 3-D nanostructure is minimal, the presence of extraneous material remaining in front of or behind the nanostructure partially obscures the nanostructure during TEM imaging. This makes atomic resolution imaging difficult due to the projection through multiple (typically amorphous) layers of material.

Another established method to analyze 3-D nanostructures such as nanowires in cross section is to mechanically scrape the nanostructures off of the sample and deposit them onto a TEM mesh grid [28]. This method is effective especially for long nanowires where some physical damage at the base of the nanowire is of no concern and site-specific information is not required. Other methods follow the general idea of physically removing the nanostructures from the substrate, often into a solution, before spreading them onto a TEM grid [29,30,31]. However, it is not possible to choose a specific nanostructure or site using these methods and it is difficult to avoid some damage to the nanostructures when mechanically removing them from the substrate.

Given the need for site-specific 3-D nanostructure analysis free of obscuring material or damage, this work focuses on the development of a wet-chemical etch process for FIB-processed TEM lamella that leaves 3-D nanostructures free of surrounding material and with ion beam damage below the detection limits of TEM for improved TEM analysis.

2. Experimental details

The nanostructures used to demonstrate this wet-chemical etch method were vertical nanopillars comprised of alternating Si/SiGe layers. Pillars of varying diameter were fabricated on commercially available 300 mm (100) Si wafers with alternating layers of 15 nm thick Si and Si_{1-x}Ge_x layers, with $x = 0.3$. With four layers each of Si and SiGe, the total Si/SiGe stack reached 120 nm in height. The pillars were defined using e-beam lithography with the Nanoscale Pattern

Generation System (NPGS) program and a continuous Bosch deep reactive ion etch, resulting in 120 nm tall pillars with diameters ranging from 25 nm to 200 nm. Center to center distances in the pillar arrays were triple that of each pillar diameter (i.e. 50 nm pillars were 150 nm apart from neighboring pillars) to prevent overdeveloping the hydrogen silsesquioxane (HSQ) resist during patterning. After pillar formation the samples were coated with ~200 nm of SiO₂ using plasma-enhanced chemical vapor deposition (PECVD) on a Unaxis 790 PECVD instrument. This oxide protected the pillars during TEM sample preparation in the FIB and allowed for subsequent removal of all surrounding material using a wet etch. Cross sections were prepared on a FEI Helios Nanolab 600 dual beam FIB/scanning electron microscope (SEM) system with Omniprobe™ capabilities. Samples were analyzed using high resolution S/TEM on a FEI Titan™ G2 80–200 STEM. The benchtop plasma cleaner used was a model GV10x plasma cleaner manufactured by ibss Group Inc. and was operated at 35 W under a pressure of approximately 5 Torr using air.

3. Cross sectional tem specimen fabrication methods

A well-established in situ lift-out method for TEM sample preparation was employed [6,24] with several key modifications that made subsequent wet-chemical etching of the cross sectional TEM lamella possible. For in situ lift-out of cross sections for TEM, samples are first protected from undesired ion implantation from the FIB by a deposited protective layer of material such as carbon. The area of interest is then additionally protected in the FIB with a platinum strap deposited first with the electron beam and then the ion beam in conjunction with the gas injection system (GIS) that provides a local platinum-based gas cloud near the sample surface [32]. Trenches are then milled on either side of the platinum strap using the ion beam to form a cross sectional lamella from the bulk sample. The sample is then tilted and undercut, either leaving the lamella lying in the trench or attached as a cantilever on one side. Next, the lamella is welded to a micromanipulator with platinum before being freed from the bulk sample via ion beam milling. Once free, the lamella is then attached to a TEM grid by platinum deposition before being released from the micromanipulator via ion beam milling. Typically, large lamellae are attached to the top of the TEM grid post (i.e. lamellae greater than approximately 50 μm long) to provide stability whereas shorter lamellae (i.e. lamellae less than 20 μm long) are able to be mounted as a “flag” on the side of the TEM grid posts. After the lamella is welded to the TEM grid, samples are thinned until electron transparent using a series of ion beam milling steps that are typically done with decreasing ion beam voltages to reduce damage and decreasing currents to increase accuracy of the milling area. During these thinning steps, the dual beam nature of the FIB/SEM system becomes especially valuable, as the user is able to monitor the ion beam milling in real time with electron beam imaging.

During final thinning, the accompanying ion beam damage is partially mitigated through use of lower voltages as the lamella is nearing completion. However, even the lowest ion beam voltages inevitably create some amount of surface damage to the sides of the lamella. This damage obscures the material of interest and prevents high-resolution microscopy. Further, damage accumulation may be especially prevalent in nanostructures [33]. The wet-chemical etch method described in this work was developed to selectively remove the surrounding material without damaging the nanostructures with the ion beam or mechanical breakage during removal of surrounding material.

Fig. 1 illustrates the wet-etch method developed for nanostructure characterization using the Si/SiGe pillars in Fig. 1A as an example material with Si shown in red, SiGe shown in blue, SiO₂ shown in yellow, Pt shown in silver, and the TEM grid shown in dark gray. The first step in the wet etch method after the nanostructures are ready for analysis is the deposition of a sacrificial SiO₂ layer as shown in Fig. 1B. The SiO₂ layer takes the place of the protective carbon coating often used during in situ FIB lift-out methods and provides protection during

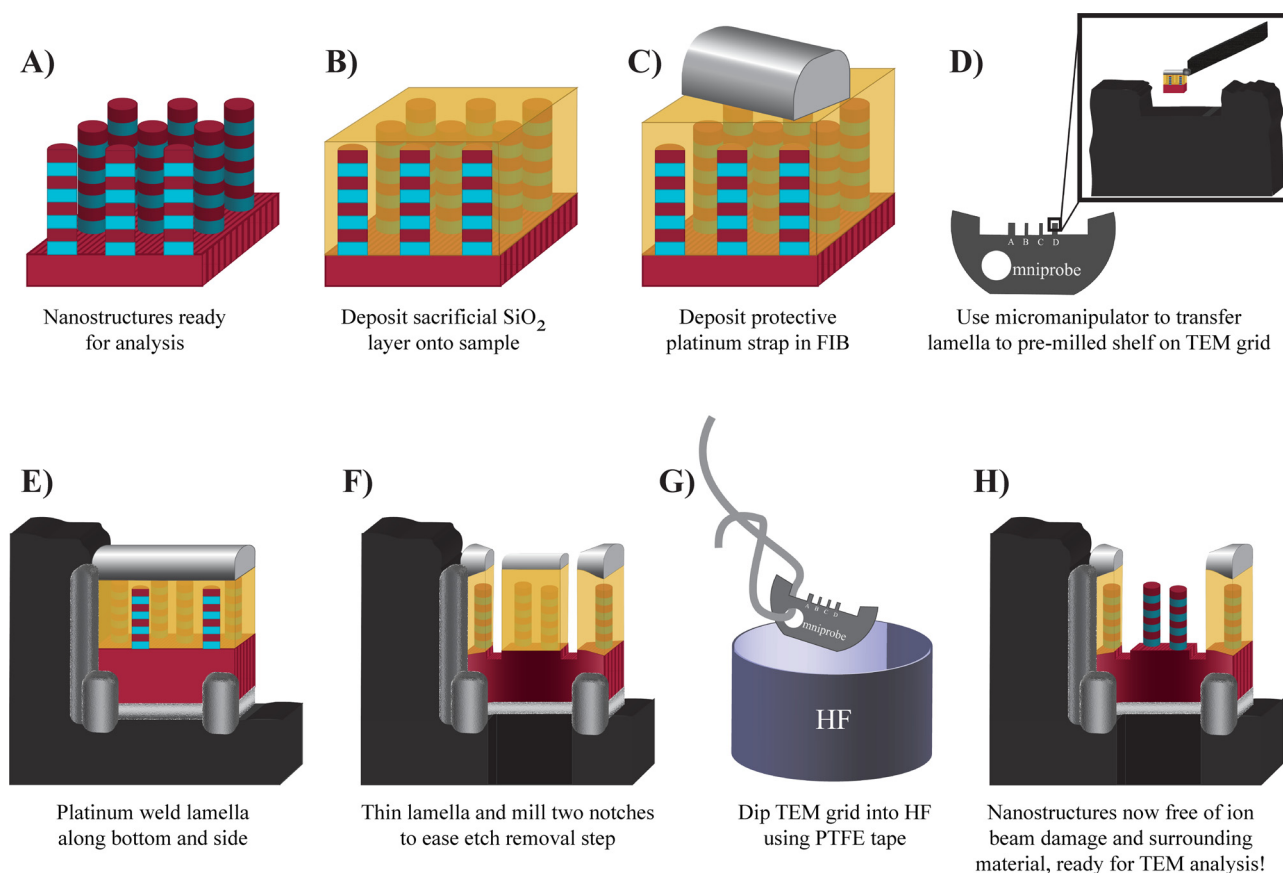


Fig. 1. A-H are cartoons that depict the key steps of the lamella fabrication process. Red represents Si, blue represents SiGe, yellow represents SiO₂, silver represents Pt, and dark gray represents the TEM grid. (For interpretation of the references to colour in this figure legend, the reader is referred to the web version of this article.)

the initial FIB platinum deposition as well as enabling the later removal of all surrounding material from the cross section. For the 120 nm tall Si/SiGe structures used to demonstrate the wet-etch method, a 200 nm layer of SiO₂ was sufficient to allow for the subsequent chemical etching release without completely removing the sample topography necessary for navigation on the sample during FIB processing. Although some charging of the surface during SEM imaging occurred, the surface charging did not prohibit the lift-out process and could likely be mitigated with an additional carbon layer on top of the SiO₂ layer if necessary. The sample is then ready for cross section fabrication using the FIB, beginning with the deposition of a protective Pt strap as shown in Fig. 1C. For the Si/SiGe pillar array, it was useful to deposit the protective platinum and mill out the lamella at a slight angle, ~2–4°, with respect to the pillar rows in order to ensure that a pillar was captured in the lamella. The procedure for milling out a cross section as described in the beginning of Section 3 is used, ending with transfer of the cross section from the sample to the TEM grid. Details of the specific FIB settings used for the fabrication of the lamellae in this work are given in Table S1 in the Supplemental Information section. Fig. 1D illustrates the necessary TEM grid modifications to ensure a strong lamella attachment to the grid.

Previous attempts at wet etching of lift-out TEM lamellae were dismissed as unsuitable due to the fragility of the lamellae. Therefore, both proper mounting of lamellae and maintaining structural durability of lamellae during thinning are critical for the successful wet-chemical etching of post-FIB process TEM lamellae. Typical flag mounting of lamellae, while efficient and effective for many material systems, will not be robust enough to withstand a wet-chemical etching process. For mounting a lamella that will undergo a wet etch, robust attachment to the TEM grid is critical. To this end, a shelf is milled at the top of the TEM post as shown in Fig. 1D before beginning the lift-out process. The

shelf must be long enough to accommodate the micromanipulator during lamella placement. Recommended shelf dimensions are approximately 10 μm tall and roughly double the length of the lamella to be mounted (i.e. a 10 μm long lamella would require a 20 μm long shelf). For this wet-chemical etch method, Mo Omniprobe® lift-out grids seem to work better than Cu lift-out grids. While slightly more expensive, Mo grids offer more resistance to bending and damage during handling which is of high value during the wet etch step. Second, because the lamella is being mounted close to the surface of the grid, it is important that the grid not redeposit material onto the lamella during final thinning. We observe very little redeposition when using Mo grids. Finally, Omniprobe® grids have a large “O” cut into the base of the grid, enabling the threading of the grid for better handling during wet etching. One downside of Mo grids is the slower milling rate for fabricating the shelf. For our Mo grid, an ion beam setting of 30 kV and 50 nA was sufficient to mill through in a timely fashion while achieving straight, flat surfaces on the grid. A lower 15 nA milling step was used to smooth the bottom and side of the shelf where the lamella would be mounted to avoid snagging of the lamella on the grid during installation. As the shelf has been ion beam milled at a 52° angle with respect to the z axis (with the stage at a zero degree tilt), it is important to mount the lamella on the “high” side of the shelf. That is, it is important to attach the lamella to the corner that is topographically highest on the grid.

Once the lamella has been navigated to the corner of the shelf, platinum is deposited to the bottom and side of the lamella nearest the grid shelf as shown in Fig. 1E. The final platinum thickness along the lamella side attachment is roughly 1 μm. Two additional tabs of platinum, also roughly 1 μm in thickness, are deposited on the bottom corners of the lamella, bracketing the area of interest.

Thinning of the lamella can also be minimized as the material

surrounding the nanostructure will be removed through the wet-chemical etch step, meaning that the thinning time for these lamella is reduced compared to other high resolution TEM samples. This method allows the user to avoid most of the time-consuming low kV cleaning steps typically necessary to reduce the damaged amorphous layers on the lamella sides. Leaving the lamella slightly thicker than typical XTEM samples also ensures that the nanostructure of interest will not be exposed to the ion beam during rough thinning of the lamella.

In order to help give the lamella the best chance of surviving a dip etch, several precautions were taken during the ion beam-thinning steps to maintain structural integrity of the mounted sample. First, the ends of the lamella where the additional platinum tabs were deposited were not thinned after mounting. Second, the total thinning of the sample was limited to what was necessary to remove obstructive sample material (i.e. other Si/SiGe pillars) in front of and behind the nanostructures of interest. It was not necessary to thin away the deposited oxide, as this would be later removed during the wet-chemical etch. For the case study with pillar diameters ranging from 200 nm to 25 nm, the final thickness of the lamella was approximately 300 nm. For other samples this final lamella thickness will vary based on the dimensions of the nanostructures of interest and the relative denseness of other structures in the surrounding area.

For the case study samples, ion beam milling at 30 kV with decreasing currents provided the necessary milling resolution to arrive at a ~ 400 nm thick lamella. Once the desired lamella thickness is reached, the stage is tilted to zero to bring the ion beam 52° with respect to the face of the lamella and two notches are milled through the protective platinum strap and slightly into the underlying substrate as shown in Fig. 1F. This provides easier release of the protective FIB Pt bar during the wet-chemical etch step. The thicker ends of the lamella often are not freed of the Pt bar as either the wet etch cannot access the middle of the deposited oxide layer or the previous ion beam milling steps have caused redeposition of milled material that blocks the oxide surface from exposure to the wet etch. Fig. 2 illustrates the results of FIB milling into the sides of the lamella for easier Pt bar release in the Si/SiGe example material. The notches are milled slightly into the substrate to ensure release during the wet-etch step.

Once the lamella is securely attached to the grid, thinned to a thickness that ensures only one nanostructure is present for a given thickness of the lamella, and notched as shown in Fig. 1F, the grid is ready to be wet etched to remove the surrounding material. Melkonyan et al. have had success in wet chemical etching atom probe tips containing fins and pillars for reduction of artefacts during atom probe evaporation, suggesting that removal of SiO_2 from 3-D nanostructures mounted using FIB techniques is a viable technique [34]. However, a novel method for securely holding the TEM grid during the wet-chemical etch is needed. TEM grids are difficult to handle due to their small

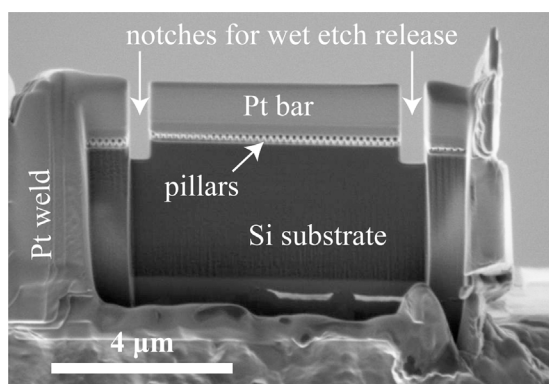


Fig. 2. SEM image of lamella after the last 30 kV thinning steps. Two notches are milled to help ease the release of the sacrificial SiO_2 layer and Pt protective bar. After this step, the ion beam voltage is decreased for final thinning of the lamella if necessary.

size and somewhat delicate nature and would be particularly difficult to hold onto with plastic tweezers during a dip etch without either bending the grid or losing the grid into the solution, especially given the personal protective equipment necessary during hydrofluoric (HF) acid use.

To address this issue, polytetrafluoroethylene (PTFE) tape was used to create an HF resistant string to hold the grid during the chemical dip as shown in Fig. 1G. It is especially helpful for this wet etch method that the Omniprobe™ TEM lift-out grids have a large "O" cut into the base of each TEM grid. To secure the grid during the wet etch, Teflon tape string was threaded through the "O" in the grid, creating a large loop with which to securely hold the grid as shown in Fig. 1G. To remove the ~ 200 nm thick sacrificial SiO_2 layer, grids were dipped into 49% HF for 30 s followed by a dip into deionized water. Grids were then allowed to dry overnight before TEM analysis. Fig. 1H shows the final result of this wet-etch method: 3-D nanostructures free of surrounding material and ready to be analyzed using TEM. Plasma cleaning should be avoided if at all possible after the wet etch of the grid as undesirable deposition of Pt particles was observed on the region of interest after plasma cleaning. This observation is discussed further in Section 4 of this work.

4. Results

The wet etch method described in this work allows for the capture of 3-D nanostructures of varying size in one lamella without needing to variably thin the lamella to each nanostructure thickness. Fig. 3 shows Si/SiGe pillars with diameters down to 25 nm to demonstrate this wet-chemical etch method, with Fig. 3A illustrating high-angle annular dark-field (HAADF) STEM imaging of a lamella with a range of Si/SiGe pillar diameters. Fig. 3A demonstrates the ability to capture a range of nanostructure sizes in one cross section without needing to variably thin the lamella to achieve electron transparency for different nanostructure thicknesses. Fig. 3B demonstrates the ability to successfully capture Si/SiGe pillars with diameters down to 25 nm. Fig. 3C provides a high resolution HAADF STEM image of a Si/SiGe pillar sidewall free of surrounding material and free of any damage observable via TEM analysis. While the wet etch method requires an additional step before and after FIB processing, the mounting and thinning of the lamella is faster as the operator doesn't need to use time-consuming low voltage ion beam cleaning steps because the outer layers of material will be removed via the wet etch. This method has a strong advantage in that site-specific imaging of 3-D nanostructures is made possible while avoiding ion beam damage during lamella lift-out and thinning.

Fig. 4 compares the S/TEM results of several cross section methods,

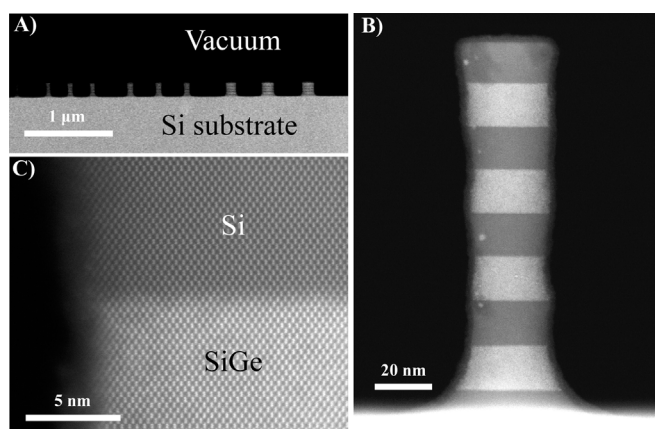


Fig. 3. Cross-sectional HAADF STEM images of Si/SiGe pillars with Si is shown in dark gray and SiGe shown in light gray. A) Low magnification image of a lamella with a range of pillar diameters for analysis. B) 25 nm diameter Si/SiGe pillar after the wet etch method. C) Sidewall of a 25 nm pillar showing atomic resolution of the Si/SiGe layers.

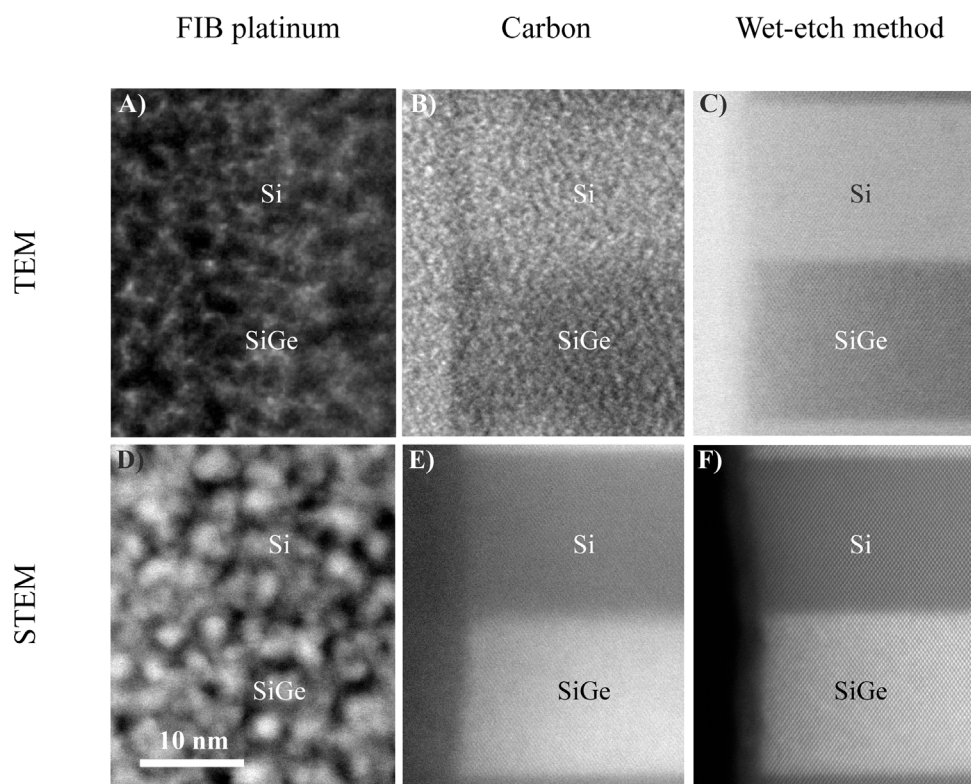


Fig. 4. TEM (A-C) and HAADF STEM (D-F) images of Si/SiGe pillars comparing the effects of Pt, C, and no surrounding material on micrograph quality. A) High resolution TEM micrograph of the Si/SiGe pillar surrounded by Pt as a result of XTEM lamella fabrication in the FIB, B) surrounded by the common FIB protective material carbon, and C) free of all surrounding material and free of TEM-detectable ion beam damage using the wet etch method outlined in this work. The bottom three micrographs demonstrate STEM analysis of the samples with D) Pt encapsulation, E) carbon encapsulation, and F) using the wet etch method.

beginning with a TEM cross section sample made using conventional FIB methods (Fig. 4A and 4D) where platinum was deposited directly onto the sample for ion beam protection. Fig. 4B and 4E show a sample where carbon was deposited to provide conduction and some protection before platinum deposition. Fig. 4C and 4F provide a final cross section fabrication comparison with a TEM cross section after removal of the surrounding material using the new etch approach described in this work. The final pillar shown after the wet etch is free of ion beam damage detectable via S/TEM analysis and free of surrounding material, allowing for clear atomic resolution TEM (Fig. 4C) and HAADF STEM (Fig. 4F) imaging of the nanostructure. Fig. 4B and 4E demonstrate that, while better than attempting to image through the platinum grains shown in Fig. 4A and 4D, a carbon protective layer still did not provide the atomic resolution of the structure available after the wet etch method. Particularly, HAADF STEM imaging through carbon still provided fairly good resolution of the layers. This may be partly due to the way HAADF STEM information is collected. While high resolution TEM detects electron interactions with the sample from the direct beam and surrounding Bragg beams resulting in phase contrast and subsequently suffers from phase distortions due to the obscuring materials (carbon or platinum in Fig. 4A and 4B) around the specimen, HAADF STEM detects electrons scattered at high angles from the sample and does not suffer from phase distortions. Elements with lower atomic numbers will scatter fewer electrons at these high angles, meaning carbon is less visible in the HAADF STEM image when compared to the TEM micrograph of the same specimen. However, when comparing Fig. 4E and 4F, we can see that the removal of the surrounding material provides the highest micrograph clarity.

Finally, plasma cleaning of the XTEM samples after the wet etch for TEM analysis resulted in the appearance of platinum particles on the surface of the pillars. Fig. 5 shows the sidewall of a Si/SiGe pillar directly after the wet etch method (Fig. 5A) and after a five minute plasma clean (Fig. 5B) in a benchtop plasma cleaner operated at 35 W at a pressure of approximately 5 torr under air. Plasma cleaning is commonly used to remove hydrocarbons from TEM sample surfaces before analysis to reduce the amount of carbon buildup during imaging.

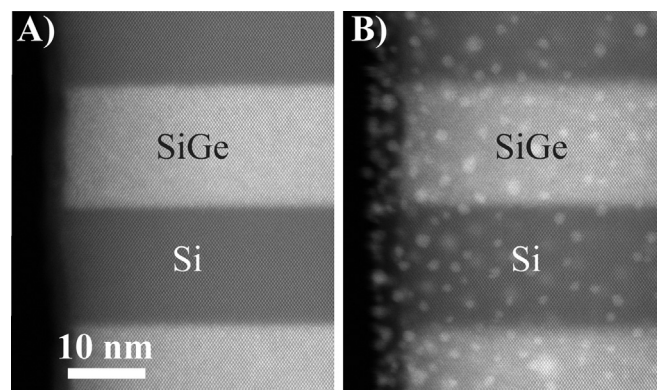


Fig. 5. HAADF STEM images of a Si/SiGe pillar A) after the wet etch method without plasma cleaning before STEM analysis. B) The Si/SiGe pillar after the wet etch method and a 5 min plasma clean, now coated with platinum particles.

Although plasma has been used to sputter platinum [35,36], plasma cleaners use a low enough energy that sputtering of material during the clean is typically not a concern. However, a dramatic increase in particulate after a plasma clean was observed and energy-dispersive spectroscopy (EDS) mapping suggested that these particles were composed of platinum. The particles may originate from sputtering (during the plasma clean) of the platinum weld used to hold the lamella to the TEM grid. It is possible that the HF wet etch attacked the organics in the organometallic FIB platinum, leaving it susceptible to sputtering during the plasma clean. For this wet etch method, it may be best to use alternate methods of TEM sample cleaning, one possibility being a vacuum oven bake to remove hydrocarbons without sputtering the FIB platinum weld onto the region of interest.

5. Conclusions

A novel approach to TEM sample preparation was discussed, demonstrating the effectiveness of removing surrounding material from 3-

D nanostructures for improved TEM resolution. It was shown that by using a protective, sacrificial, encapsulating material and making small alterations to the lift-out and mounting FIB procedures, routine wet-chemical etching of TEM lamella is possible and provides a route to removing material that obscures the cross sectional TEM view of 3-D nanostructures while leaving the nanostructures free of FIB ion beam damage detectable by TEM analysis during fabrication of the lamella.

Declaration of Competing Interest

The authors declare that they have no known competing financial interests or personal relationships that could have appeared to influence the work reported in this paper.

Funding

This work was supported by the Laboratory Directed Research and Development program at Sandia National Laboratories, a multimission laboratory managed and operated by National Technology and Engineering Solutions of Sandia, LLC., a wholly owned subsidiary of Honeywell International, Inc., for the U.S. Department of Energy's National Nuclear Security Administration under contract DE-NA-0003525. This work was performed, in part, at the Center for Integrated Nanotechnologies, a U.S. Department of Energy, Office of Basic Energy Sciences user facility. This paper describes objective technical results and analysis. Any subjective views or opinions that might be expressed in the paper do not necessarily represent the views of the U.S. Department of Energy or the United States Government

Supplementary materials

Supplementary material associated with this article can be found, in the online version, at doi:10.1016/j.ultramic.2020.113049.

References

- [1] S. Reyntjens, R. Puers, A review of focused ion beam applications in microsystem technology, *J. Micromechanics Microengineering* 11 (2001) 287–300.
- [2] M.J. Vasile, R. Nassar, J. Xie, Focused ion beam technology applied to microstructure fabrication, *J. Vac. Sci. Technol. B Microelectron. Nanom. Struct.* 16 (1998) 2499–2505.
- [3] T. Sakamoto, Z. Cheng, M. Takahashi, M. Owari, Y. Nihei, Development of an Ion and Electron Dual Focused Beam Apparatus for Three-Dimensional Microanalysis, *Japanese J. Appl. Physics, Part 1 Regul. Pap. Short Notes Rev. Pap.* 37 (1998) 2051–2056.
- [4] T.J. Steer, G. Möbus, O. Kraft, T. Wagner, B.J. Inkson, 3-D focused ion beam mapping of nanoindentation zones in a Cu-Ti multilayered coating, *Thin Solid Films* 413 (2002) 147–154.
- [5] F. Lenrick, M. Ek, D. Jacobsson, M.T. Borgström, L.R. Wallenberg, FIB Plan and Side View Cross-Sectional TEM Sample Preparation of Nanostructures, *Microsc. Microanal.* 20 (2014) 133–140.
- [6] R.M. Langford, A.K. Petford-Long, Preparation of transmission electron microscopy cross-section specimens using focused ion beam milling, *J. Vac. Sci. Technol. A* 19 (5) (2001) 2186–2193.
- [7] C. Li, G. Habler, L.C. Baldwin, R. Abart, An improved FIB sample preparation technique for site-specific plan-view specimens: a new cutting geometry, *Ultramicroscopy* 184 (2018) 310–317.
- [8] D. Tomus, H.P. Ng, In situ lift-out dedicated techniques using FIB – SEM system for TEM specimen preparation, *Micron* 44 (2013) 115–119.
- [9] R. Wirth, Focused Ion Beam (FIB) combined with SEM and TEM: advanced analytical tools for studies of chemical composition, microstructure and crystal structure in geomaterials on a nanometre scale, *Chem. Geol.* 261 (2009) 217–229.
- [10] M. Simon-najasek, S. Huebner, F. Altmann, A. Graff, Advanced FIB sample preparation techniques for high resolution TEM investigations of HEMT structures, *Microelectron. Reliab.* 54 (2014) 1785–1789.
- [11] A. Denisjuk, T. Hrnčíř, J. Vincenc Oboňa, M. Petreenc Sharang, J. Michalička, Mitigating Curtaining Artifacts During Ga FIB TEM Lamella Preparation of a 14 nm FinFET Device, *Microsc. Microanal.* 23 (2017) 484–490.
- [12] P. Longo, H. Zhang, R.D. Twesten, Simultaneous DualEELS and EDS analysis across the ohmic contact region in 3D NAND storage and FinFET electronic devices, *Mater. Sci. Semicond. Process.* 65 (2017) 44–48.
- [13] V. Pott, K.E. Moselund, D. Bouvet, L. De Michielis, A.M. Ionescu, Fabrication and Characterization of Gate-All-Around Silicon Nanowires on Bulk Silicon, *IEEE Trans. Nanotechnol.* 7 (6) (2008) 733–744.
- [14] H. Trombini, et al., Unraveling structural and compositional information in 3D FinFET electronic devices, *Sci. Rep.* 9 (2019) 11629.
- [15] M. Spies, A. Ajay, E. Monroy, B. Gayral, M.I. den Hertog, Correlated Electro-Optical and Structural Study of Electrically Tunable Nanowire Quantum Dot Emitters, *Nano Lett* 20 (2020) 314–319.
- [16] X.T. Zhou, J.Q. Hu, C.P. Li, D.D.D. Ma, C.S. Lee, S.T. Lee, Silicon nanowires as chemical sensors, *Chem. Phys. Lett.* 369 (2003) 220–224.
- [17] L. Chen, F. Cai, U. Otunoye, W.D. Lu, Vertical Ge/Si Core/Shell Nanowire Junctionless Transistor, *Nano Lett* 16 (2016) 420–426.
- [18] B.-H. Lee, et al., A Vertically Integrated Junctionless Nanowire Transistor, *Nano Lett* 16 (2016) 1840–1847.
- [19] A.-M. Siladie, et al., Mg and In Codoped p-type AlN Nanowires for pn Junction Realization, *Nano Lett* 19 (2019) 8357–8364.
- [20] J. Mayer, L.A. Giannuzzi, T. Kamino, J. Michael, TEM Sample Preparation and FIB-Induced Damage, *MRS Bull.* 32 (2007) 400–407.
- [21] D.B. Williams, C.B. Carter, *Transmission Electron Microscopy*, Springer, New York, 2009.
- [22] K.A. Mkhoyan, S.E. Maccagnano-Zacher, E.J. Kirkland, J. Silcox, Effects of amorphous layers on ADF-STEM imaging, *Ultramicroscopy* 108 (8) (2008) 791–803.
- [23] T. Grieb, et al., Quantitative HAADF STEM of SiGe in presence of amorphous surface layers from FIB preparation, *Ultramicroscopy* 184 (2018) 29–36.
- [24] M. Schaffer, B. Schaffer, Q. Ramasse, Sample preparation for atomic-resolution STEM at low voltages by FIB, *Ultramicroscopy* 114 (2012) 62–71.
- [25] N.I. Kato, Y. Kohno, H. Saka, Side-wall damage in a transmission electron microscopy specimen of crystalline Si prepared by focused ion beam etching, *J. Vac. Sci. Technol. A Vacuum, Surfaces, Film.* 17 (4) (1999) 1201–1204.
- [26] S. Hata, H. Sosiati, N. Kuwano, M. Itakura, T. Nakano, Y. Umakoshi, Removing focused ion-beam damages on transmission electron microscopy specimens by using a plasma cleaner, *J. Electron Microsc. (Tokyo)*. 55 (1) (2006) 23–26.
- [27] Z. Huang, Combining Ar ion milling with FIB lift-out techniques to prepare high quality site-specific FIB samples, *J. Microsc.* 215 (3) (2004) 219–223.
- [28] S. Ashrafabadi, H. Eshghi, Synthesis and characterization of n-type lightly doped mesoporous silicon nanowires through 1-MACE, influence of etching solution temperature, *J. Mater. Sci. Mater. Electron.* 29 (2018) 6470–6476.
- [29] S.H. Moosavi, M. Kroener, M. Frei, F. Frick, S. Kerzenmacher, P. Woias, Development of a TEM Compatible Nanowire Characterization Platform With Self-Forming Contacts, *IEEE Trans. Semicond. Manuf.* 31 (1) (2018) 22–31.
- [30] M. Mohl, et al., Formation of CuPd and CuPt bimetallic nanotubes by galvanic replacement reaction, *J. Phys. Chem. C* 115 (2011) 9403–9409.
- [31] B. Pramanick, A. Salazar, S.O. Martinez-Chapa, M.J. Madou, Carbon TEM grids fabricated using C-MEMS as the platform for suspended carbon nanowire characterization, *Carbon N. Y.* 113 (2017) 252–259.
- [32] T. Tao, J. Ro, J. Melngailis, Z. Xue, H.D. Kaesz, Focused ion beam induced deposition of platinum, *J. Vac. Sci. Technol. B Microelectron. Nanom. Struct.* 8 (6) (1990) 1826–1829.
- [33] J.A. El-Awady, C. Woodward, D.M. Dimiduk, N.M. Ghoniem, Effects of focused ion beam induced damage on the plasticity of micropillars, *Phys. Rev. B - Condens. Matter Mater. Phys.* 80 (10) (2009) 104104.
- [34] D. Melkonyan, et al., Wet-chemical etching of atom probe tips for artefact free analyses of nanoscaled semiconductor structures, *Ultramicroscopy* 186 (2018) 1–8.
- [35] A. Caillard, P. Brault, J. Mathias, C. Charles, R.W. Boswell, T. Sauvage, Deposition and diffusion of platinum nanoparticles in porous carbon assisted by plasma sputtering, *Surf. Coatings Technol.* 200 (2005) 391–394.
- [36] T. Shibano, K. Nakamura, T. Oomori, Platinum etching in Ar/O₂ mixed gas plasma with a thin SiO₂ etching mask, *J. Vac. Sci. Technol. A Vacuum, Surfaces, Film.* 16 (2) (1998) 502–508.